In vivo quantitation of rare circulating tumor cells by multiphoton intravital flow cytometry

Wei He*, Haifeng Wang†, Lynn C. Hartmann‡, Ji-Xin Cheng*†, and Philip S. Low*§

*Department of Chemistry and †Weldon School of Biomedical Engineering, Purdue University, West Lafayette, IN 47907; and ‡Division of Medical Oncology, Mayo Clinic, Rochester, MN 55905

Edited by Mark T. Groudine, Fred Hutchinson Cancer Research Center, Seattle, WA, and approved May 31, 2007 (received for review April 30, 2007)

Quantitation of circulating tumor cells (CTCs) constitutes an emerging tool for the diagnosis and staging of cancer, assessment of response to therapy, and evaluation of residual disease after surgery. Unfortunately, no existing technology has the sensitivity to measure the low numbers of tumor cells (<1 CTC per ml of whole blood) that characterize minimal levels of disease. We present a method, intravital flow cytometry, that noninvasively counts rare CTCs *in vivo* as they flow through the peripheral vasculature. The method involves i.v. injection of a tumor-specific fluorescent ligand followed by multiphoton fluorescence imaging of superficial blood vessels to quantitate the flowing CTCs. Studies in mice with metastatic tumors demonstrate that CTCs can be quantitated weeks before metastatic disease is detected by other means. Analysis of whole blood samples from cancer patients further establishes that human CTCs can be selectively labeled and quantitated when present at ≈2 CTCs per ml, opening opportunities for earlier assessment of metastatic disease.

folate conjugates | *in vivo* imaging | multiphoton microscopy | metastasis | cancer diagnosis

The decision to administer chemotherapy after tumor resection usually depends on an oncologist's assessment of the presence of microscopic metastatic disease. Although computed tomography, MRI, tissue/sentinel lymph node biopsy, and serum cancer marker analysis can all detect some level of residual disease, the presence of circulating tumor cells (CTCs) is reported to correlate most sensitively with cancer progression and metastasis (1, 2). Measurement of CTCs, however, remains difficult, with most methods relying on quantitation of cells expressing epithelial markers after their isolation from peripheral blood samples (1–6). Noninvasive imaging of these CTCs in real time as they flow through the peripheral vasculature could improve detection sensitivity by enabling analysis of significantly larger blood volumes (potentially the entire blood volume of the patient), but to date such analyses have proven successful only when cancer cells are labeled *ex vivo* before their i.v. injection (7, 8). Although mitochondria-containing cells and apoptotic cells have been successfully labeled *in vivo* for detection in the vasculature (9, 10), no method has yet been developed for *in vivo* labeling and quantitation of CTCs. Here we design and optimize such a method using modified multiphoton intravital microscopy.

Results

Evaluation and Optimization of the Methods for *in Vivo* Imaging of CTCs. Recent estimates suggest that many human carcinomas overexpress a receptor for the vitamin folic acid (>90% of ovarian and endometrial cancers, 86% of kidney cancers, 78% of nonsmall cell lung cancers, etc.) (11–17). In contrast, normal tissues either lack measurable folate receptors (FR) or express FR at a site that is inaccessible to parenterally administered drugs. Because FR-expressing cancer masses can be selectively labeled *in vivo* by injection of either radioactive or fluorescent folate conjugates that bind FR with nanomolar affinity (18), we wondered whether single CTCs might bind sufficient numbers of folate conjugates to allow their detection *in vivo* as they pass through a patient's peripheral vasculature. To first identify the optimal method for such detection, we compared the abilities of nonconfocal, confocal, and multiphoton fluorescence microscopy to detect 1,1′-dioctadecyl-3, 3,3′,3′-tetramethylindocarbocyanine perchlorate [$DiIC_{18}$ (3)]-labeled RBCs in circulation after their injection into the tail veins of live mice. Analysis of both signal-to-background ratio and number of cells detected per minute revealed that multiphoton microscopy was moderately more sensitive than confocal microscopy, with nonconfocal microscopy significantly inferior to either method (Table 1 and Fig. 1*a*). Because of its superior sensitivity, as well as its improved tissue penetration and reduced propensity for photodamage (19, 20), multiphoton microscopy was selected for all subsequent studies. Further, to significantly enhance the speed of data acquisition (a modification essential for capturing CTCs in rapidly flowing blood vessels), customary two-dimensional scanning was changed to one-dimensional line scanning along a transept orthogonal to the flow of blood in the monitored vessel. This change improved the rate of data acquisition 250-fold (21).

To further increase signal-to-background ratios, a tumor-specific probe had to be selected that would rapidly clear from circulation if left uncaptured by CTCs. After multiple comparisons, folate-dye conjugates were selected over fluorescent antibodies, not only because labeled antibodies circulate for days before their removal, thereby causing significant problems with background fluorescence, but also because tumor-specific antibodies were found to promote phagocytic clearance of the CTCs to which they bound, thereby causing significant underestimation of CTC counts (8), as shown in the studies below. However, to ensure that folate conjugates would clear sufficiently rapidly from circulation to enable CTC imaging, we injected various folate-dye conjugates i.v. at doses of 5 nmol per mouse and monitored their depletion kinetics by intravital time-lapse fluorescence microscopy. As shown in Fig. 1*b*, plasma clearance of folate-rhodamine was biphasic, with a rapid phase characterized by a $t_{1/2}$ of ≈3–5 min and comprising 75% of the clearance in anesthetized mice and a slower phase that we attribute to serum protein binding. Because these data are similar to those reported for folate-FITC (22, 23), we assume that folate-dye conjugates will generally be rapidly excreted if they are not captured by a FR-expressing cell.

To explore whether cancer cells can be selectively labeled with folate conjugates in whole blood, whole blood samples from three healthy donors were spiked with nasopharyngeal cancer cells (KB) that were first labeled *in vitro* with the lipophilic dye, DiD (1,1′-dioctadecyl-3,3,3′,3′-tetramethylindodicarbocyanine, 4-chloroben-

Author contributions: W.H., L.C.H., J.-X.C., and P.S.L. designed research; W.H. and H.W. performed research; W.H. contributed new reagents/analytic tools; W.H. analyzed data; and W.H., L.C.H., J.-X.C., and P.S.L. wrote the paper.

The authors declare no conflict of interest.

This article is a PNAS Direct Submission.

Abbreviations: CTC, circulating tumor cells; FR, folate receptor; $DiIC_{18}$ (3), 1,1′-dioctadecyl-3, 3,3′,3′-tetramethylindocarbocyanine perchlorate.

§To whom correspondence should be addressed at: Department of Chemistry, Purdue University, 560 Oval Drive, West Lafayette, IN 47907. E-mail: plow@purdue.edu.

www.pnas.org/cgi/doi/10.1073/pnas.0703875104

Table 1. Comparison of nonconfocal, confocal, and multiphoton fluorescence scanning microscopy for *in vivo* sensing of $DiIC_{18}$(3)-labeled RBCs

Parameter measured	Nonconfocal	Confocal	Multiphoton
Output power, mW*	1	1	35
Background intensity, a.u.	492–651	47–108	15–47
Signal intensity, a.u.	786–3,895	337–1,588	204–3,895
S/B ratio	1.30–6.98	3.46–21.90	5.51–108.90
S/B mean	2.36 ± 0.96†	9.37 ± 4.37†	22.38 ± 14.52†
Number detected, cells/min‡	124.0 ± 13.2†	54.8 ± 8.8†	100.0 ± 11.1†

S/B, signal-to-background ratio.
*Output power was measured as the laser power out of objective lens.
†Values are expressed ± SD.
‡Number detected represents the number of cells detected by two-photon fluorescence microscopy.

zenesulfonate), to allow their tracking. The spiked blood samples were then treated with 100 nM folate-AlexaFluor 488 and analyzed by flow cytometry for the presence of both DiD and AlexaFluor 488. Importantly, virtually all DiD-labeled cancer cells were found to be simultaneously labeled with folate-AlexaFluor 488 (Table 2). More importantly, no fluorescent cells were detected in any blood samples lacking cancer cells (data not shown), confirming that the low level of FR expression on activated monocytes (≈60,000 per cell) is too low for detection with intravital flow cytometry.

***In Vivo* Imaging and Quantitation of CTCs in Murine Cancer Models.** We next introduced L1210A leukemia cells (10^6) i.v. into BALB/c mice to mimic the occurrence of natural CTCs. Fifteen minutes later, folate-rhodamine (5 nmol per mouse) was administered i.v. to label the CTCs, and after an additional 30 min to allow for clearance of unbound conjugates, multiphoton intravital microscopy was used to detect circulating L1210A cells in the vasculature of the ear. One example of an L1210A cell captured in three consecutive frames over a period of 1 s is shown in Fig. 1*c*. To confirm that such cells were indeed CTCs, we labeled the L1210A cells with DiD before introducing them into mice and performing the *in vivo* labeling as mentioned above (only in this case, labeling was conducted with folate-FITC to avoid fluorescent crosstalk with DiD). Importantly, folate-FITC was found to label only DiD-positive cells, as exemplified in the representative overlay image of one CTC shown in Fig. 1*d*. For more quantitative analysis of these CTCs in larger, faster-flowing vessels, fluorescence scanning was reduced to a single dimension along a transept perpendicular to the vessel. This modification allowed an increase in scan rate from 2 to 500 frames

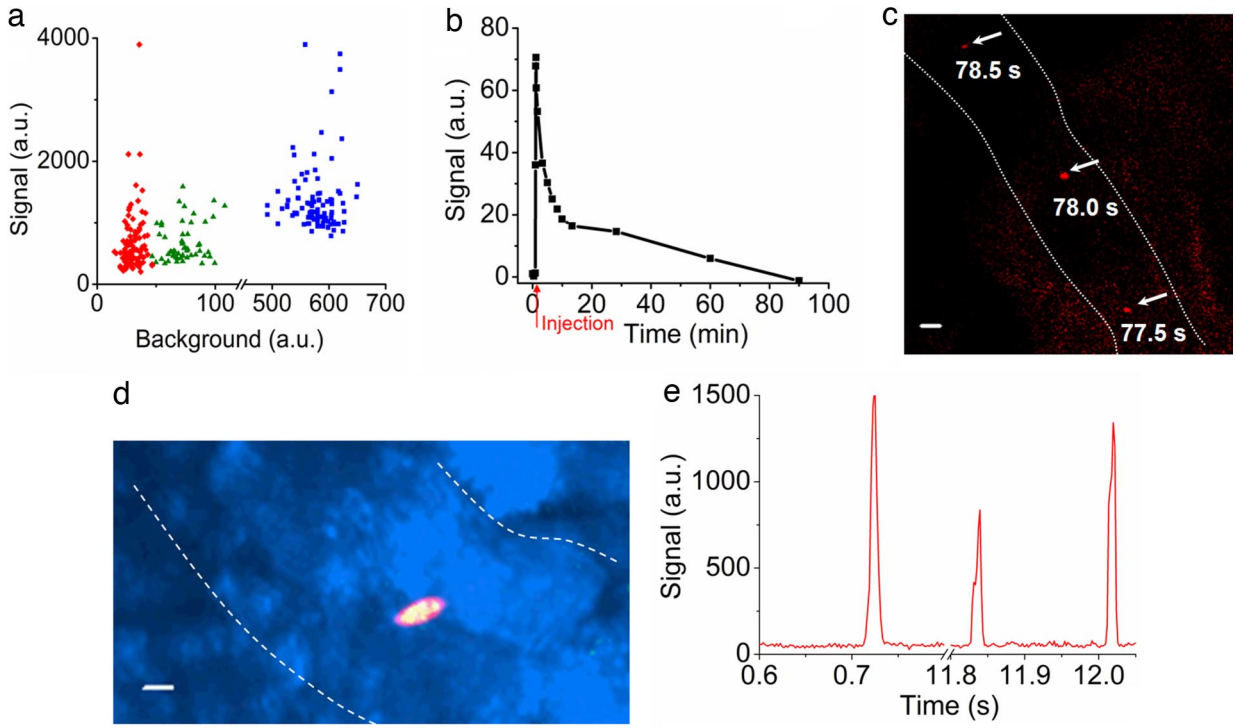

Fig. 1. Optimization of *in vivo* detection of fluorescent cells in circulation. (*a*) Dot plot of signal and background intensities of individual fluorescent $DiIC_{18}$ (3)-labeled RBCs flowing through the vasculature in the ear of a live mouse, as determined by multiphoton (red, $n = 107$), confocal (green, $n = 55$), and nonconfocal (blue, $n = 100$) microscopy. (*b*) Kinetics of the clearance of folate-rhodamine from circulation in anesthetized mice. Red arrow marks the injection point. (*c*) Overlay image of three consecutive frames spanning 1 s showing an *in vivo* folate-rhodamine-labeled L1210A cell traveling in a blood vessel. (*d*) Specificity of *in vivo* labeling of L1210A tumor cells with folate-FITC demonstrated by the overlap (yellow) of folate-FITC (green) and DiD (red) fluorescence. (*e*) Visualization of digitized signals of fluorescent L1210A cells labeled *in vivo* with folate-FITC and detected/analyzed by one-dimensional line scanning using software developed on MATLAB platform. (Scale bars: *c* and *d*, 10 μm.) Dotted lines outline blood vessel walls identified by transillumination in *c* and *d*.

Table 2. Evaluation of the efficiency of labeling cultured cancer cells added to whole human blood with folate conjugates

No. of cancer cells in 1 ml of blood	Efficiency of detection, %		
	Donor 1	Donor 2	Donor 3
10	100.0	100.0	100.0
10^2	100.0	100.0	100.0
10^3	100.0	99.2	100.0
10^4	99.8	99.8	99.6
10^5	99.8	99.6	99.7
Mean*	99.92 ± 0.11	99.72 ± 0.33	99.86 ± 0.19

*The mean (± SD) represents the average labeling efficiency of folate conjugates in the whole blood from three different healthy donors.

per s. Derived digitized signals obtained by this method were then processed by using software developed on the MATLAB platform and found to yield signal to background ratios >8:1 (Fig. 1*e*).

To study whether CTCs originating from a primary solid tumor could be quantitated *in vivo* before metastatic disease was detectable by microscopic examination of necropsied tissues, a metastatic tumor model was established by s.c. implanting M109 murine lung cancer cells with moderate FR expression on the dorsal flanks of BALB/c mice. By 2 weeks after implantation, ≈1.4 CTCs per min could be detected in the vasculature of the ear, whereas by 3 and 4 weeks after implantation, ≈7 and 18 CTCs per min, respectively, were measured (Fig. 2 *a* and *b*). Indeed, CTC counts increased exponentially with tumor growth. To determine when metastatic nodules might become visible in the same animals, the mice were euthanized after *in vivo* imaging, and tissue sections (draining lymph nodes, lungs, kidneys, spleen, liver, bone marrow, etc.) were examined by both immunohistochemical staining and fluorescence confocal microscopy. No evidence of metastatic disease was found in any tissues during the first 4 weeks after tumor implantation, however, a few micrometastases could be detected in the lungs (dimensions <50 × 30 × 30 μm) at week 5. Thus, CTCs were readily quantitated in circulation weeks before evidence of metastatic nodules could be found in necropsied tissue sections.

Flow Cytometric Assay of Blood Samples from Ovarian Cancer Patients. To investigate whether natural CTCs from cancer patients can be labeled with sufficient folate conjugates to permit their detection in whole blood, fresh blood samples collected in heparin from 12 ovarian cancer patients with various pathologies (patients 1–5, 8, and 10–12: stage III; patient 6: stage I; patient 7: stage II; patient 9: stage IV) were treated with 100 nM folate-AlexaFluor 488 and then examined by flow cytometry. As shown in Fig. 2*c*, except for patients 6 and 7, who had early-stage cancers, all patients displayed CTC counts significantly greater than background (<6 CTCs per ml). In contrast, similar samples from three healthy donors were found to contain no CTCs per ml (data not shown). To further ensure that the cells labeled with folate-AlexaFluor 488 were indeed malignant, the peripheral blood samples from patients 1–5 were labeled with monoclonal anti-human CA125 antibody plus the appropriate secondary antibody conjugated to rhodamine-X. As shown in Fig. 2*d*, the green fluorescence of folate-AlexaFluor 488 was only found on cells labeled with rhodamine-X, demonstrating that the folate-AlexaFluor-labeled cells indeed derive from ovarian cancer.

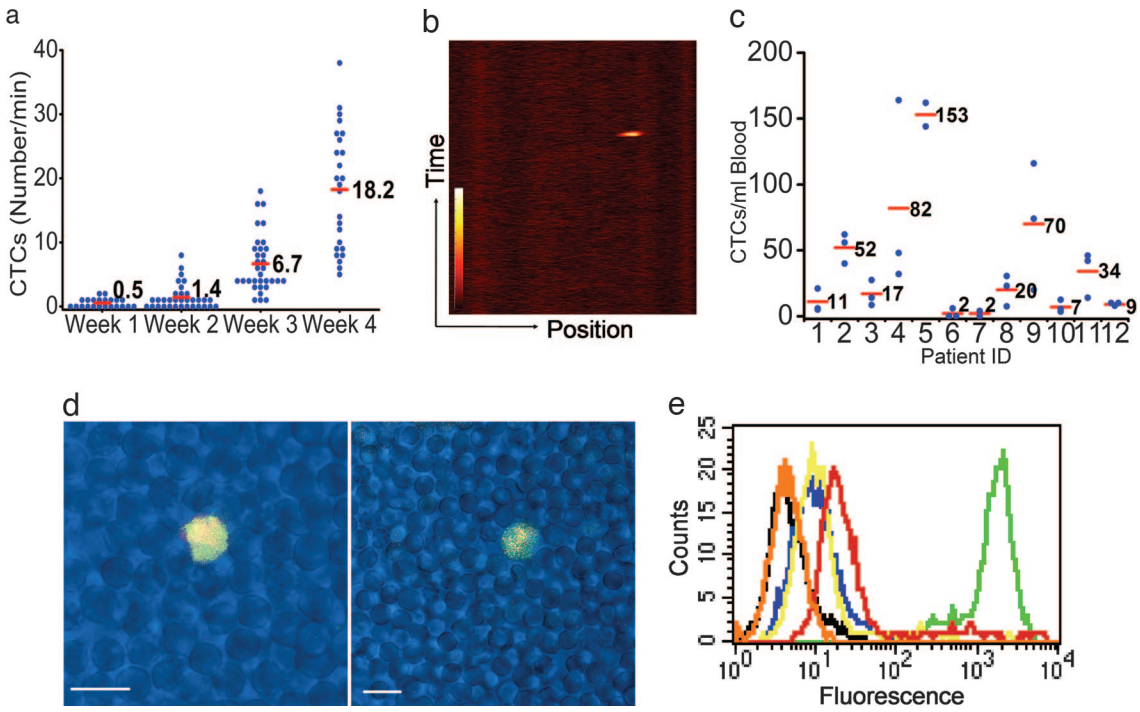

Fig. 2. Quantitation of CTCs by both *in vivo* imaging of animal models and *ex vivo* flow cytometry of peripheral blood samples from ovarian cancer patients. (*a*) Change in CTCs as a function of time after M109 tumor cell implantation. CTCs were quantitated by measuring the number of fluorescent tumor cells per minute flowing through a blood vessel in the ear of each mouse. Red bars represent mean values. (*b*) Method of image processing. One thousand line scans, spanning a 2-s time period, across a blood vessel are combined sequentially by using MATLAB software to yield the displayed image. (*c*) CTC counts in peripheral blood samples from 12 ovarian cancer patients with different pathologies. Red bars represent mean values from multiple independent measurements. (*d*) Confocal images of single CTC in blood smears from an ovarian cancer patient. Overlap of green (folate-AlexaFluor 488) with red (rhodamine-X-labeled anti-cytokeratin antibody) fluorescence is displayed as yellow fluorescence. (Scale bar: 10 μm.) (*e*) Comparison of the labeling intensities of folate-FITC (green) and three different polyclonal anti-FR antibodies conjugated with FITC: PU9 (red), PU10 (yellow), and PU17 (navy). Unlabeled KB cells (black) and KB cells incubated with 10 μM folic acid plus 100 nM folate-FITC (orange, totally competed) serve as negative controls.

Evaluation of Fluorescent Antibodies as Labeling Agents. Finally, as mentioned above, antibody-based probes, including three distinct polyclonal antibodies against FR, were also tested for their abilities to identify rare CTCs *in vivo*. Curiously, no CTCs could be detected in tumor-bearing mice after i.v. administration of any tumor-specific antibody. This failure to detect CTCs by using antibodies was not expected (data not shown), especially because the antibodies were labeled with multiple copies of fluorescein (in contrast to folate which was always linked to a single fluorescein or another fluorescent molecule). To explain these data, we hypothesized that our inability to detect CTCs might have arisen from either a failure of the antibodies to bind CTCs *in vivo* or a rapid antibody-promoted clearance of the opsonized CTCs by phagocytic cells (8). To explore the former mechanism, we examined the capabilities of three different FITC-conjugated anti-FR-specific polyclonal antibodies to label FR^+ KB cells *in vitro*. Although all three antibodies were found to immunoblot FR in the KB cell extracts at >1:20,000 dilution, their abilities to stain KB cells *in vitro* was found to be >100-fold lower than folate-FITC (Fig. 2*e*). It is conceivable that this difference in labeling efficiency might relate to the relative sizes of folate-FITC (M_r = 881) versus antibodies (M_r = ≈160,000) and their relative accessibilities to FR on the CTC surface. Whether antibody labeling of the CTCs *in vivo* also contributed to their rapid removal by the reticuloendothelial system was not investigated.

Discussion

The above data were all obtained by using folate as the targeting ligand. Because not all cancers express FR, use of folate-dye conjugates to detect recurrent disease in the clinic will necessarily be limited to those patients whose primary tumors demonstrate FR expression during initial immunohistochemical analysis of their resected tumors. Detection of FR^- tumors must then depend on development of analogous high-affinity ligands that are specific for other cancers, as reported in the literature (24, 25).

Current *in vivo* diagnostic imaging technologies such as computed tomography, MRI, and positron-emission tomography can detect micrometastases only to a resolution of ≈2–3 mm (26). To permit earlier detection of metastatic disease, an *in vitro* diagnostic test, based on magnetic bead sorting followed by immunostaining and fluorescence imaging, has been recently developed that can detect ≈5 CTCs in 7.5 ml of human peripheral blood (1, 2). Although this improvement in detection sensitivity will likely save lives, its usefulness is limited by the volume of blood that can be sampled, thereby compromising CTC detection during the initial phases of metastasis, in early stages of disease, or when CTC numbers are reduced by therapy. In contrast, intravital flow cytometry circumvents sampling limitations and renders quantitation of rare events (<1 CTC per ml) statistically significant by enabling analysis of the majority of a patient's blood volume (≈5 liters).

Folate-dye conjugates were also found to enable quantitation of CTCs in smaller blood volumes (2 ml) by conventional *ex vivo* flow cytometry. Although *ex vivo* flow cytometry has the advantage that detected cells (*i*) can be further characterized by forward and side light scattering and (*ii*) can be sorted and subsequently studied by other methods, it also suffers from the small sample size mentioned above as well as the possible introduction of human errors during sample preparation. Nevertheless, where CTC concentrations in the blood are high, *ex vivo* flow cytometry should still constitute the preferred method because of the common availability of the necessary instrumentation. However, even for *ex vivo* CTC analyses, data in Fig. 2*e* demonstrate that sensitivity can be greatly improved (≈100-fold) by substitution of folate-dye conjugates for fluorescently labeled antibodies.

Despite the aforementioned advantages of intravital flow cytometry, several challenges remain before the methodology can be implemented in the clinic. First, because an average 70-kg cancer patient will have ≈5 liters of blood, interrogation of the patient's entire blood volume will require at least ≈1 h assuming the blood vessel under observation has a diameter of 3 mm and flows at a rate of ≈100 ml/min (27). Although it can be argued that a patient's entire blood volume need not be interrogated, methods will still have to be developed to maintain the desired blood vessel in focus for the desired duration of the assay. Second, folate-dye conjugates must be shown to be completely nontoxic before they can achieve routine use in the clinic. Although folate-FITC (2.7 mmol/kg) is currently being administered i.v. to cancer patients with no discernable toxicity (folate-hapten immunotherapy) (National Institutes of Health clinical trial: Safety and Tolerability Study of FolateImmune in Combination with Cytokines in Patients with Refractory or Metastatic Cancer, clinical trial identifier: NCT00329368; see also ref. 28), none of the other folate-dye conjugates has been tested in humans. However, because the concentration of folate-FITC used to detect CTCs in tumor-bearing mice (Fig. 2*a*) is 10-fold lower than that currently used in the above clinical trial, we anticipate that folate-labeling agents will generally be well tolerated. Third, consumption of high doses of folic acid could conceivably raise serum folate concentrations to levels that compete with folate-dye conjugates for binding to CTCs (29, 30). Although no constraints were placed on vitamin utilization by the cancer patients tested in Fig. 2*c*, it is conceivable that abstinence from vitamin supplements for 24 h before CTC analysis might have further improved the sensitivity of the assay. Indeed, cancer patients to be scanned with a folate-linked ^{111}In radioimaging agent were asked to refrain from folic acid supplements for 24 h before image collection (31). Such restrictions could conceivably improve the signal-to-noise ratio seen in Fig. 1*e*. Finally, cancer patients have been frequently shown to have measurable levels of anti-FR antibodies in their sera (32). Although these antibodies could conceivably reduce folate-dye conjugate binding to cancer cells, we have no data to suggest that they compete with folate conjugates for FR. Rather, because >200 cancer patients have been successfully imaged with a folate-linked radioimaging agent, we believe that interference from anti-FR antibodies must be minimal, if present at all.

Although further optimization of the intravital flow cytometry assay is warranted, the fact that CTC detection was successful with multiple folate-dye conjugates (folate-rhodamine, folate-FITC, and folate-AlexaFluor 488) on multiple cancer cells (KB, M109, L1210A, and natural CTCs in ovarian cancer patients) suggests that there is flexibility in the methodology if changes should be necessary. Because better tools for the diagnosis and staging of cancer, assessment of response to therapy, and evaluation of residual disease after surgery can save lives, we suggest that optimization of the methodology for human use is worth pursuing. Finally, it should also be noted that high-affinity, low-molecular-weight ligands with specificities for other rare populations of pathologic cells (e.g., bacteria, viruses, parasites, and activated immune cells) can be similarly designed and synthesized for related applications.

Materials and Methods

Reagents. $DiIC_{18}$ (3), Vybrant DiD cell-labeling solution, fluorescein isothiocyanate, anti-CA125 antibodies, and corresponding secondary antibodies conjugated to rhodamine-X were purchased from Invitrogen (Eugene, OR). Ficoll-Paque was purchased from Amersham (Piscataway, NJ). Rabbit anti-FR antisera from three separate rabbits, affinity columns, and folate-FITC were provided by Endocyte, Inc (West Lafayette, IN).

Mice. All experimental protocols were approved by the Purdue University Animal Care and Use Committee. For the identification of the optimal imaging method, blood was collected from anesthetized mice by paraorbital extraction in heparin. RBCs were then isolated, labeled by DiI_{18} (3), and injected i.v. for the optimization experiment as described below (33).

In vivo imaging experiments were carried out on 6- to 8-week-

old female BALB/c mice (Harlan Labs, San Diego, CA) fed a folate-deficient chow for at least 2 weeks. Because commercial chow is supplemented with very high levels of folic acid, mice fed on this chow have serum folate concentrations near 700 nM (34, 35), a value >50 times greater than normal. We have found that 2–3 weeks of exposure to folate-deficient chow is sufficient to lower murine serum folates to a level (≈20 nM) comparable to that of human serum (29, 34–36). When desired, anesthesia was performed by i.p. injection of Avertin (500 mg/kg). Each anesthetized animal was placed in a chamber with its ear taped to the bottom of the dish by using double-faced tape.

L1210A and M109 cells were cultured in folate-deficient RPMI 1640 (Gibco, Rockville, MD) for several weeks to up-regulate FR expression to levels commonly found in ovarian cancers ($\approx 3 \times 10^6$ FR per cell) (17). At the time of tumor implantation, L1210A and M109 cells expressed $\approx 3.5 \times 10^6$ and 1×10^6 FR per cell, respectively. For the L1210A tumor model, 10^6 L1210A cells were injected through one of the lateral tail veins, and 20 min later, 5 nmol per mouse of folate-rhodamine was injected through the other tail vein. For specificity studies, L1210A cells were labeled *ex vivo* with DiD before tail vein injection. Mice were then treated i.v. with 5 nmol of folate-FITC and imaged as stated above. For the M109 metastatic cancer model, 5×10^5 passage 0 or 1 (P_0 or P_1) M109 cells isolated from a s.c. tumor were implanted s.c. on the back of the mouse. Folate-rhodamine (5 nmol per mouse) was injected through the tail vein for *in vivo* labeling. Microscopic necropsy, H&E pathological examination, and immunohistochemistry were carried out by veterinary pathologists at the Animal Disease Diagnostic Laboratory of Purdue University to identify metastatic sites in different organs.

Flow Cytometry. To evaluate the labeling efficiency of folate conjugates in human whole blood, fresh blood was obtained from three healthy donors in heparinized tubes and spiked with different numbers (10–10^5/ml) of DiD-labeled KB cells (a human nasopharyngeal cell line). The blood samples were then incubated with 100 nM folate-AlexaFluor 488 for 30 min at 37°C before analysis by flow cytometry. Efficiency of detection was calculated by dividing the number of folate-AlexaFluor 488-positive cells by the number of DiD-positive cells.

To quantitate CTC levels in blood samples from patients with ovarian cancer, whole blood samples in anticoagulant were obtained under the auspices of an Institutional Review Board-approved protocol at the Mayo Clinic. Each patient's sample was separated into four 500-μl aliquots, three of which were incubated with 100 nM folate-AlexaFluor 488 at 37°C for 30 min, and the fourth was first incubated with 10 μM folic acid for 30 min at 37°C before the above incubation with 100 nM folate-AlexaFluor 488. This fourth sample served as a nonspecific binding control. FR^+ cells were then counted by using appropriate gates and controls by flow cytometry.

For comparison of the labeling efficiencies of folate-FITC with three FITC-labeled anti-FR antibodies, cultured KB cells were incubated for 30 min at 37°C with each of the above probes before analysis by flow cytometry. Unlabeled KB cells and KB cells incubated with 10 μM unconjugated folic acid before addition of 100 nM folate-FITC (totally competed) served as negative controls.

Immunocytochemistry. The patient blood samples were treated with folate conjugates as stated above. After labeling, CTCs were enriched by Ficoll-Paque density centrifugation separation and labeled with primary anti-CA125 antibodies and appropriate secondary antibodies conjugated with rhodamine-X. The treated samples were then washed and examined by confocal fluorescence microscopy.

Folate Conjugates and Antibody Conjugates. Folate conjugates were synthesized as reported in the literature (37, 38). Anti-FR polyclonal antibodies, PU9, PU10, and PU17, were purified by affinity column chromatography and transferred to PBS (pH 9.0) for conjugation. Fluorescent labeling was carried out at a ratio of 80 μg of FITC per milligram of antibody at room temperature for 4 h in the dark. After conjugation, labeled antibodies were purified by affinity chromatography and transferred to PBS (pH 7.4). Antibody concentration and FITC-to-protein ratio were calculated by using the following formula, which is based on IgG and FITC absorbance values: concentration (mg/ml) = $[A\ (280) - 0.31 \cdot A\ (495)]/1.4$, FITC-to-protein ratio = $3.1 \cdot A\ (495)/[A\ (280) - 0.31 \cdot A\ (495)]$.

***In Vivo* Imaging.** *In vivo* imaging of $DiIC_{18}$ (3)-labeled RBCs was conducted on a laser-scanning microscope (IX70/FV300; Olympus, Tokyo, Japan) that was modified to permit rapid interconversion between nonconfocal, confocal, and two-photon excitation fluorescence (TPEF) imaging. A 543-nm He-Ne laser was used for one-photon excitation, whereas a femtosecond Ti:Sapphire laser (Mira900; Coherent, Santa Clara, CA) was used for two-photon excitation. The Ti:Sapphire laser had a 78-MHz repetition rate and 200-fs pulse duration. A ×40 IR water-immersion objective (1-UM568; Olympus) with a working distance of 3.3 mm and numerical aperture of 0.8 was used to focus the laser onto a vessel in the mouse ear. Fluorescence was collected through the same objective and filtered with either a HQ520 nm/40 nm bandpass filter (Chroma, Brattleboro, VT) for FITC detection or a 600 nm/65 nm filter (Ealing Catalog, Rocklin, CA) for rhodamine detection. For imaging L1210A cells labeled with both folate-FITC and DiD (a 670 nm/40 nm filter was used when DiD was imaged), the same laser was tuned to 790 nm. The epifluorescence was measured with photomultiplier tube (PMT) detectors (R3896; Hamamatsu, Bridgewater, NJ). For imaging folate-rhodamine, the Ti:Sapphire laser was tuned to 730 nm with 80-mW output at the objective lens. To further improve the signal-to-background ratio, an external PMT (H7422–40; Hamamatsu) was used for *in vivo* imaging of CTCs.

Image Processing. $DiIC_{18}$ (3)-labeled RBCs were injected into the tail veins of BALB/c mice and imaged *in vivo* by time-lapse microscopy by using each of the indicated methods. The signal and background fluorescence intensities and signal-to-background (S/B) ratios were quantified on single cells by using FlowView software (Olympus; version 4.3) as they passed under the scanner. Statistics (average and standard deviation) were derived from six time series images spanning 1 min for each imaging technique. All comparisons of nonconfocal ($n = 744$), confocal ($n = 600$), and multiphoton ($n = 329$) microscopy were performed on the same blood vessel by changing the optical setup while the mouse remained anesthetized.

For analysis of folate-rhodamine blood clearance kinetics, two-dimensional scans were recorded every 5 s. Blood vessel fluorescence intensities were quantified in each image by calculating the mean fluorescence by using the FlowView software (Olympus; version 4.3). For quantitation of CTCs, digitized signals collected during one-dimensional line scanning were exported and then analyzed by programming on MATLAB 7.0 platform. High-frequency noise was eliminated with a fast Gaussian filter, and the processed digitized data were imported into Origin 7.0 for visual presentation of fluorescent cells.

We appreciate Yuehui Ouyang for assistance in the development of software, Nikki Parker for antibody purification, Kimberly Kalli for her

help in organizing the collection and handling of blood samples, and Andrew Hilgenbrink (Vanderbilt University, Nashville, TN) for synthesizing folate-AlexaFluor 488. We also thank Frank Prendergast for his advice and support. We are also grateful for use of facilities at the Bindley Bioscience Center (Purdue University). This work was supported by Indiana Elks Charities Grant 671-1393-4523, the Purdue University Cancer Center, and an Ovar'Coming Cancer Together Research Grant.

1. Cristofanilli M, Budd GT, Ellis MJ, Stopeck A, Matera J, Miller MC, Reuben JM, Doyle GV, Allard WJ, Terstappen LW, *et al.* (2004) *N Engl J Med* 351:781–791.
2. Cristofanilli M, Hayes DF, Budd GT, Ellis MJ, Stopeck A, Reuben JM, Doyle GV, Matera J, Allard WJ, Miller MC, *et al* (2005) *J Clin Oncol* 23:1420–1430.
3. Allard WJ, Matera J, Miller MC, Repollet M, Connelly MC, Rao C, Tibbe AGJ, Uhr JW, Terstappen1 LW (2004) *Clin Cancer Res* 10:6897–6904.
4. Molnar B, Ladanyi A, Tanko L, Sreter L, Tulassay Z (2001) *Clin Cancer Res* 7:4080–4085.
5. Muller V, Stahmann N, Riethdorf S, Rau T, Zabel T, Goetz A, Janicke F, Pantel K (2005) *Clin Cancer Res* 11:3678–3685.
6. Wirtschafter A, Benninger MS, Moss TJ, Umiel T, Blazoff K, Worsham MJ (2001) *Arch Otolaryngol Head Neck Surg* 128:40–43.
7. Georgakoudi I, Solban N, Novak J, Rice WL, Wei X, Hasan T, Lin CP (2004) *Cancer Res* 64:5044–5047.
8. Novak J, Georgakoudi I, Wei X, Prossin A, Lin CP (2004) *Optics Lett* 29:77–79.
9. Zhong CF, Ye JY, Norris TB, Thomas T, Cao Z, Myc A, Baker JR (2005) *Lasers Electro-Optics* 3:2145–2147.
10. Wei X, Sipkins DA, Pitsillides CM, Novak J, Georgakoudi I, Lin CP (2005) *Mol Imaging* 4:415–416.
11. Weitman SD, Lark RH, Coney LR, Fort DW, Frasca V, Zurawski VR, Jr, Kamen BA (1992) *Cancer Res* 52:3396–3401.
12. Ross JF, Chaudhuri PK, Ratnam M (1994) *Cancer* 73:2432–2443.
13. Boerman OC, van Niekerk CC, Makkink K, Hanselaar TG, Kenemans P, Poels LG (1991) *Int J Gynecol Pathol* 10:15–25.
14. Weitman SD, Weinberg AG, Coney LR, Zurawski VR, Jennings DS, Kamen BA (1992) *Cancer Res* 52:6708–6711.
15. Garin-Chesa P, Campbell I, Saigo PE, Lewis JL, Jr, Old LJ, Rettig WJ (1993) *Am J Pathol* 142:557–567.
16. Siegel BA, Dehdashti F, Mutch DG, Podoloff DA, Wendt R, Sutton GP, Burt RW, Ellis PR, Mathias CJ, Green MA, Gershenson DM (2003) *J Nucl Med* 44:700–707.
17. Parker N, Turk MJ, Westrick E, Lewis JD, Low PS, Leamon CP (2005) *Anal Biochem* 338:284–293.
18. Leamon CP, Low PS (1991) *Proc Natl Acad Sci USA* 88:5572–5576.
19. So PTC, Dong CY, Masters BR, Berland KM (2000) *Annu Rev Biomed Eng* 2:399–429.
20. Zipfel WR, Williams RM, Webb WW (2003) *Nat Biotechnol* 21:1369–1377.
21. Im KB, Han S, Park H, Kim D, Kim BM (2005) *Opt Express* 13:5151–5156.
22. Leamon CP, Parker MA, Vlahov IR, Xu LC, Reddy JA, Vetzel M, Douglas N (2002) *Bioconjugate Chem* 13:1200–1210.
23. Paulos CM, Reddy JA, Leamon CP, Turk MJ, Low PS (2004) *Mol Pharmacol* 66:1406–1414.
24. Bugaj JE, Achilefu S, Dorshow RB, Rajagopalan R (2001) *J Biomed Opt* 6:122–133.
25. Foss CA, Mease RC, Fan H, Wang Y, Ravert HT, Dannals RF, Olszewski RT, Heston WD, Kozikowski AP, Pomper MG (2005) *Clin Cancer Res* 11:4022–4028.
26. Benaron DA (2002) *Cancer Met Rev* 21:45–78.
27. Talegón-Meléndez A, Ciria-Lloréns G, Gómez-Cía T, Mayo-Iscar A (1999) *J Ultrasound Med* 18:553–558.
28. Lu Y, Low PS (2002) *Cancer Immunol Immunother* 51:153–162.
29. Jacques PF, Selhub J, Bostom AG, Wilson PWF, Rosenberg IH (1999) *N Engl J Med* 340:1449–1454.
30. Morris MS, Jacques PF, Rosenberg IH, Selhub J (2007) *Am J Clin Nutr* 85:193–200.
31. Siegel BA, Dehdashti F, Mutch DG, Podoloff DA, Wendt R, Sutton GP, Burt RW, Ellis PR, Mathias CJ, Green MA, *et al.* (2003) *J Nucl Med* 44:700–707.
32. Knutson KL, Krco CJ, Erskine CL, Goodman K, Kelemen LE, Wettstein PJ, Low PS, Hartmann LC, Kalli KR (2006) *J Clin Oncol* 24:4254–4261.
33. Hillery CA, Du MC, Montgomery RR, Scott JP (1996) *Blood* 87:4879–4886.
34. Mathias CJ, Wang S, Lee RJ, Waters DJ, Low PS, Green MA (1996) *J Nucl Med* 37:1003–1008.
35. NIH Molecular Imaging and Contrast Agent Database. Available at: http://www.ncbi.nlm.nih.gov/books/bv.fcgi?rid=micad.chapter.Folate-DF-Ga. Accessed April 1, 2007.
36. Reddy JA, Xu L-C, Parker N, Vetzel M, Leamon CP (2004) *J Nucl Med* 45:857–866.
37. Kennedy MD, Jallad K, Lu J, Low PS, Ben-Amortz D (2003) *Pharm Res* 20:714–719.
38. Sandoval RM, Kennedy MD, Low PS, Molitoris BA (2004) *Am J Physiol* 287:C517–C526.